Computation of Seismic Soil-Structure Interaction with Mixed Implicit-Explicit Scheme

D. Aubry, D. Chouvet

Ecole Centrale des Arts et Manufactures, Grande voie des vignes, F-92290 Chatenay-Malabry, France

SUMMARY

In this paper results on dynamic earthpressures against a retaining wall are presented. This problem is directly linked with a stability analysis and requires thus the development of an elastoplastic equation for the soil valid even with large lagrangian deformations. The subsequent soil-structure interaction problem is efficiently implemented with a finite element technique coupled with a mixed scheme for the time integration : the structure is implicitely integrated while the soil is treated explicitely. The whole process is finally validated against experimental results on a scaled model constituted of walls of different sizes and shapes and retaining a granular medium, the ensemble being submitted to strong shakings of different characteristics. A computer code has been implemented and it is thus possible to assess the validity of the assumptions of simplified procedures such as those derived from Mononobe equations. Finally the technique may be directly extended to the dynamic stability of slopes and earthdams.

1. INTRODUCTION

The problem of dynamic earthpressures and of the stability of retaining walls has been studied most often with simplified well-known procedures [1], and has scarcely been studied as a classical dynamic soil-structure interaction problem like e.g. surface foundations. Furthermore a stability analysis is very often used for this problem requiring a study of large anelastic deformations.

The aim of this paper is to present such an analysis for an elastoplastic soil with finite plastic deformations. The equations of the model will be detailed in the first paragraph. The subsequent equations are highly nonlinear and it is at first sight tempting to implement an explicit scheme for the numerical computation. However the stiffness of the wall may be very high compared to the stiffness of the strained backfill so that the time step required to insure the stability of the numerical scheme may be very low. In order to circumvent this difficulty which is typical of many interaction problems a mixed algorithm is used : the soil is explicitely integrated while the wall is implicitely treated. For the discretization of the space variables a classical finite element technique is used. The proposed scheme is detailed in the second paragraph and its efficiency is then discussed.

It is natural to think that a sophisticated procedure must be carefully validated. As seismic events have usually not been enough instrumented, it has been decided to perform experiments on scaled models with different types of seismic sollicitations. The comparisons of the numerical results with those provided by the experiments are very encouraging and are examined in the last part.

2. DERIVATION OF THE EQUATIONS.

We consider here a lagrangian formulation for the equilibrium equations. Let Ω denote the initial configuration of the body, and x be the cartesian coordinates in Ω. The displacement field is $u(x,t)$. The body, initially at rest, is submitted to body forces $g(x,t)$. At time t, the deformation gradient $F(u)$ is equal to $I + \nabla u$, where ∇ is the gradient operator relative to x. The inverse of $F(u)$ is denoted by $G(u)$. Let σ be the Piola-Kirchhoff stress tensor relative to Ω and ρ the corresponding mass density. The dynamic equilibrium equations are :

$$\operatorname{div}\,(F(u).\sigma) + g(x,t) = \rho\,\frac{\partial^2 u(x,t)}{\partial t^2} \qquad (1)$$

According to the theory of Mandel [2] for finite elastoplasticity with infinitesimal elastic strains, the constitutive equations are written in an intermediate configuration which is deduced from the current one by the rotation R. Let π be the Piola-Kirchhoff stress tensor relative to this intermediate configuration.

$$\sigma = |F(u)|\; G(u).R.\pi.R^T.G(u)^T \equiv T(\Sigma,\nabla u) \qquad (2)$$

Let α be the internal variables, the state of a material point of the body at time t is characterized by $\Sigma = (\pi,\alpha,R)$. As schown elsewhere [3], the evolution of this state Σ according to the elastoplastic constitutive equations may be summarized by the following evolution equation :

$$\dot{\Sigma} = H(\Sigma,\nabla u,\nabla\dot{u}) \qquad (3)$$

The integral $\int_\Omega a.b\, dx$ is denoted by the dot product $(a,b)_\Omega$. v and Θ designate virtual displacements and virtual state fields. Then the variationnal formulation is written :

$$\left[\begin{array}{l} \text{Find } u(t) \in U(\Omega),\ \Sigma(t) \in \Lambda(\Omega) \\ (\rho\ddot{u},v)_\Omega + (F(u).\sigma,\nabla u)_\Omega = (g,v)_\Omega\ ,\ \forall\ v \in U(\Omega) \\ (\dot{\Sigma},\Theta)_\Omega = (H(\Sigma,\nabla u,\nabla\dot{u}),\Theta)_\Omega\ ,\ \forall\ \Theta \in \Lambda(\Omega) \end{array}\right. \tag{4}$$

3. IMPLICIT-EXPLICIT ALGORITHM

As we already noticed in the finite element analysis of soil-structure interaction, it could be of interest to use a mixed time-integration scheme. Thus we split the domain Ω into two parts Ω_I and Ω_E, we assume that elements belonging to Ω_I and Ω_E are respectively treated implicitely and explicitely. Then following Hughes et al. [4], an implicit-explicit algorithm is written for finite deformations, starting from the well-known Newmark's algorithm. The time discretization is performed on the interval $[0,T]$, assuming a constant time step Δt. Let n be the time step number, the displacements are discretized as follows :

$$\left[\begin{array}{ll} u^*_{n+1} = u_n + \Delta t\ \dot{u}_n + \Delta t^2(1-2\beta)\ddot{u}_n & ,\quad \dot{u}^*_{n+1} = \dot{u}_n + \Delta t(1-\gamma)\ddot{u}_n \\ u_{n+1} = u^*_{n+1} + \beta\ \Delta t^2\ \ddot{u}_{n+1} & ,\quad \dot{u}_{n+1} = \dot{u}^*_{n+1} + \gamma\ \Delta t\ \ddot{u}_{n+1} \end{array}\right. \tag{5}$$

Thus the set of equations (4) is written :

$$\left[\begin{array}{l} (\frac{\rho}{\beta\Delta t^2}u_{n+1},v)_\Omega = (g_{n+1},v)_\Omega + (\frac{\rho}{\beta\Delta t^2}u^*_{n+1},v)_\Omega - (F(u^*_{n+1}).\sigma^*_{n+1},\nabla v)_{\Omega_E} - (F(u_{n+1}).\sigma_{n+1},\nabla v)_{\Omega_I} \\ (\Sigma^*_{n+1}-\Sigma_n,\Theta)_{\Omega_E} = (H(\Sigma^*_{n+1},\nabla u^*_{n+1},\nabla(u^*_{n+1}-u_n)),\Theta)_{\Omega_E} \quad , \quad \sigma^*_{n+1} = T(\Sigma^*_{n+1},\nabla u^*_{n+1}) \\ (\Sigma_{n+1}-\Sigma_n,\Theta)_{\Omega_I} = (H(\Sigma_{n+1},\nabla u_{n+1},\nabla(u_{n+1}-u_n)),\Theta)_{\Omega_I} \quad , \quad \sigma_{n+1} = T(\Sigma_{n+1},\nabla u_{n+1}) \end{array}\right. \tag{6}$$

The set of equations (6) is highly nonlinear, we use an iterative process to solve it. Let j be the iteration number, and let us introduce some useful notations :

$$m_\alpha(w,v) = (\frac{\rho}{\beta\Delta t^2}\ w,v)_{\Omega_\alpha}\ ,\ \alpha = I\ ,\ E \quad ; \quad m(w,v) = m_I(w,v) + m_E(w,v)$$

$$c_\alpha(w,s,v) = (F(w).s,\nabla v)_{\Omega_\alpha}\ ,\ \alpha = I\ ,\ E$$

$$b(w,v) = m(w,v) + (C:\varepsilon(w),\nabla v)_{\Omega_I}$$

$$r^j_{n+1}(v) = (g_{n+1},v)_\Omega + m(u^*_{n+1}-u^j_{n+1},v) - c_E(u^*_{n+1},\sigma^*_{n+1},v) - c_I(u^j_{n+1},\sigma^j_{n+1},v)$$

$b(w,v)$ denotes a symetric bilinear form, where the second part is the elastic virtual work of the implicit subdomain Ω_I. C is the elasticity tensor and $\varepsilon(w)$ is the strain measure equal to $\{\nabla w\}_s$. The different steps of the algorithm are as follows :

Step 1. Let u_n, $\dot{u}_n$, $\ddot{u}_n$, Σ_n be known. Compute u^*_{n+1}, $\dot{u}^*_{n+1}$. For j=0 , $u^\circ_{n+1} = u_n$, $\Sigma^\circ_{n+1} = \Sigma_n$

Step 2. Predictor phase on Ω_E for Σ^*_{n+1} and σ^*_{n+1} according to eq. (6b). Compute $r^\circ_{n+1}(v)$ on Ω.

Step 3. Solve for u^{j+1}_{n+1} on Ω : $b(u^{j+1}_{n+1} - u^j_{n+1},v) = r^j_{n+1}(v)$

Step 4. Solve for Σ^{j+1}_{n+1} on Ω_I : $(\Sigma^{j+1}_{n+1}-\Sigma_n,\Theta)_{\Omega_I} = (H(\Sigma^{j+1}_{n+1},\nabla u^{j+1}_{n+1},\nabla(u^{j+1}_{n+1}-u_n),\Theta)_{\Omega_I}$

Compute $\sigma^{j+1}_{n+1} = T(\Sigma^{j+1}_{n+1},\nabla u^{j+1}_{n+1})$ on Ω_I and $r^{j+1}_{n+1}(v)$ on Ω.

Step 5. Tests for convergence on u_{n+1}^{j+1} and r_{n+1}^{j+1} according to fixed tolerances DTOL and RTOL

$$|| u_{n+1}^{j+1} - u_{n+1}^{j} || \leq \text{DTOL } ||u_{n+1}^{j+1}|| \quad \text{and} \quad ||r_{n+1}^{j+1}|| \leq \text{RTOL}.||r_{n+1}^{\circ}||$$

$j = j+1$ and go to step 3 if convergence is not reached.

Step 6. Solution for displacements on Ω :

$u_{n+1} = u_{n+1}^{j+1}$, $\ddot{u}_{n+1} = (u_{n+1}-u_{n+1}^{*})/\beta\Delta t^2$, $\dot{u}_{n+1} = \dot{u}_n + \Delta t(1-\gamma)\ddot{u}_n + \beta\Delta t\ \ddot{u}_{n+1}$

Corrector phase on Ω_E, solve for Σ_{n+1}: $(\Sigma_{n+1}-\Sigma_n,\Theta)_{\Omega_E} = (H(\Sigma_{n+1},\nabla u_{n+1},\nabla(u_{n+1}-u_n),\Theta)_{\Omega_E}$

Update Σ_{n+1} on Ω_I : $\Sigma_{n+1} = \Sigma_{n+1}^{j+1}$

To take advantage of the implicit-explicit scheme, it is of utmost interest to have a consistant form $m_I(w,v)$ and a diagonal form $m_E(w,v)$ according to the finite element discretization. Thus during iterations, the values of u_{n+1}^{j+1} are constant and equal to u_{n+1}^{1} on Ω_E, the unknowns u_{n+1} are iteratively approched by u_{n+1}^{j+1} on the nodes belonging to Ω_I and to the interface. The state Σ_{n+1} is predicted by Σ_{n+1}^{*} on Ω_E at step 2 and is kept constant during iterations, it is corrected at step 6. On Ω_I the state Σ_{n+1} is iteratively approched by Σ_{n+1}^{j+1} at step 4.

We have not performed a stability analysis for this scheme. But based on numerical experiments it seems that the recommandations of Hughes are sufficient, however to prevent instability of the solution due to the high nonlinearity of the equations the convergence tolerances must be stringent enough. All the calculations presented below have been performed with the derived trapezoidal rule scheme ($\gamma = 1/2$, $\beta = 1/4$).

4. COMPARISON WITH EXPERIMENTS ON A SCALED MODEL

Experiments on scaled models have been performed in the laboratory to study the soil retaining wall system during seismic events. The model is a box 1.00 m long, 0.60 m high, 0.06 m wide, filled with rods material upon which a model of retaining wall is laid. The box is shaken at its base by an hydraulic MTS system, so that different seismic inputs are obtained. A gravity retaining wall and a cantilever wall were tested.

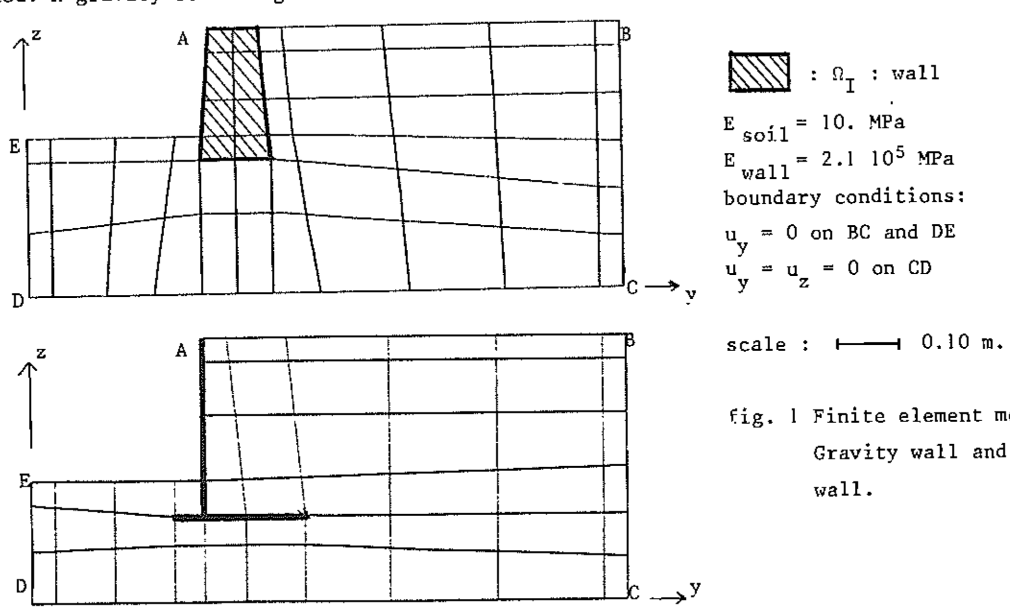

fig. 1 Finite element meshes Gravity wall and cantilever wall.

The bidimensionnal finite element mesh is regular with only a few fine elements where large deformations are experimentaly observed. Eight nodes isoparametric elements with a 2x2 Gauss integration are used (fig. 1). The constitutive equations for the soil are derived from a CamClay model with a bidimensionnal special formulation. The soil is explicitely treated while the wall is implicitely integrated. The initial state of stresses in the soil was obtained by a static computation with incremental gravity. The time step imposed by stability criteria is 5.10^{-5}s. The experimental excitations are recorded at the base of the box, two samples of accelerogram data are schown in fig.2 : a synthetical seismic accelerogram, an harmonic one, time durations are respectively 2.5s and 0.5s. The excitation is uniform all over the box, so that for the computation the system is submitted to an inertia force computed with those accelerogram data.

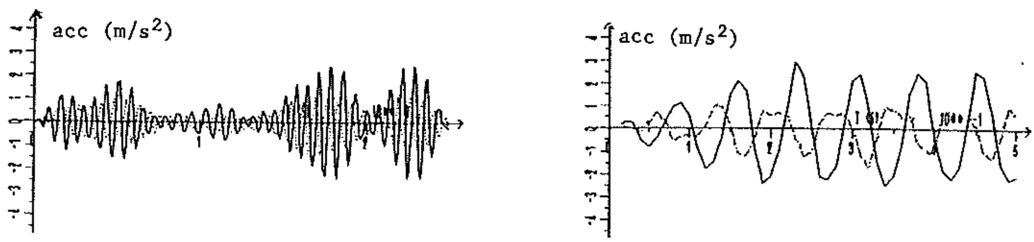

synthetical accelerogram   harmonic accelerogram

fig. 2 Accelerogram data versus time (—— horizontal, - - - - vertical)

Experimental data are compared to calculated results for the displacements and the accelerations at the top of the gravity retaining wall submitted to seismic synthetical sollicitation (fig. 3) :

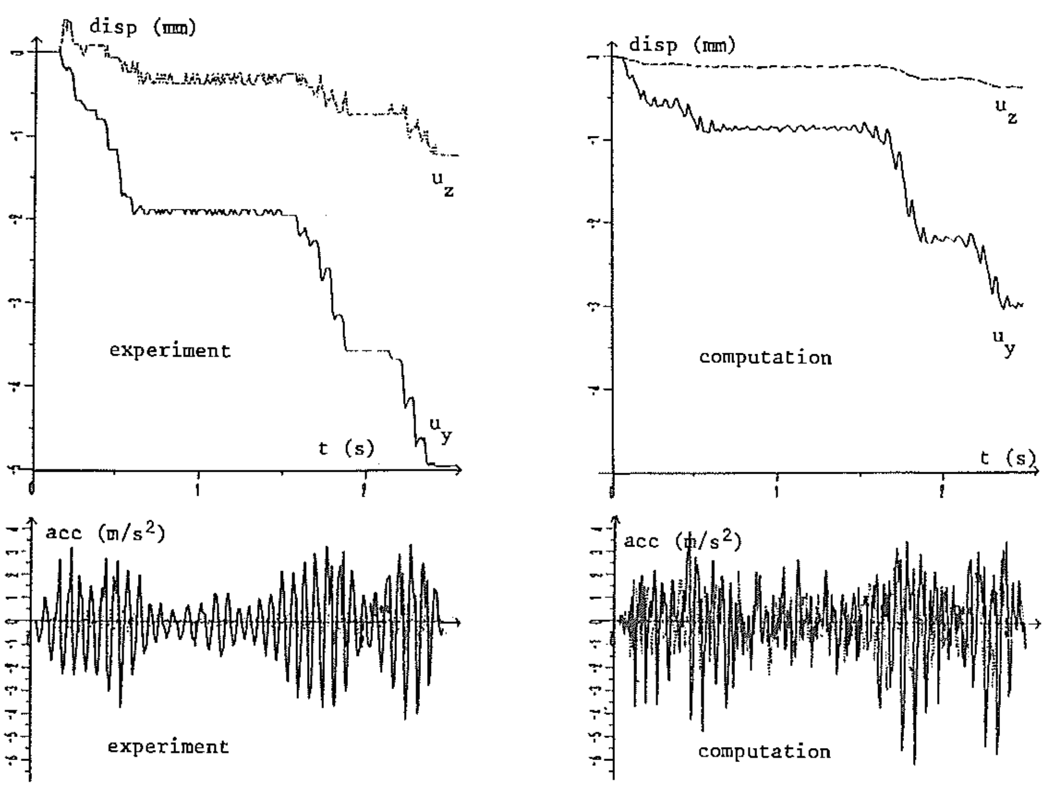

The cantilever wall submitted to the harmonic excitation gave us the experimental and computed displacements at the top of the wall schown in fig. 4.

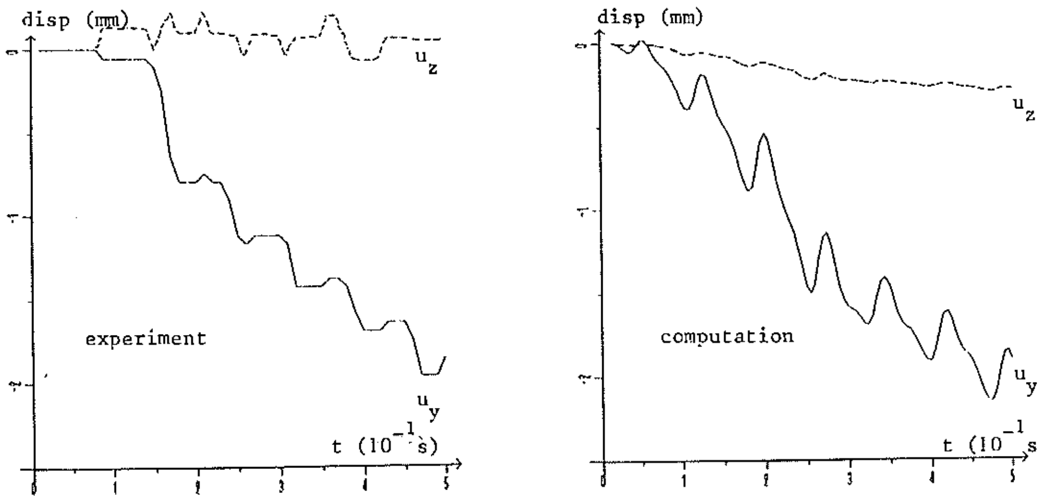

fig. 4 Experimental and computed displacements at the top of the cantilever wall

The shape of the displacements are quite different with the two types of sollicitations, the harmonic acceleration give a regular response of the wall, while under seismic acceleration the wall moves by fits and starts. The computed displacements are closed to the experimental data, the comparison for the accelerations is also quite good. The good correlation between experiments and computations is confirmed by other comparaisons for different tests [3].

We present now computationnal results on the total dynamic pressure against the gravity wall submitted to the seismic motion (fig. 5), this point having been often adressed at by other simplified methods. The total force is increasing above the static value, the large movements of the wall apart from the backfill correspond to large values of this force and maxima of its inclination on the back of the wall. With those movements the maximum of the soil-wall friction ϕ is mobilized, thus the corresponding inclination of the force with horizontal is equal to $\phi+\beta$ (β is the inclination of the back of the wall with vertical). The location of the application of the resultant force is quite constant and equal to the static value which is at one third of the height from the base of the wall.

In fig. 6 we present the total computed force acting on the fixed right side BC of the box during the same experiment. Contrary to the movable wall the dynamic force is oscillating around the static value, the large accelerations generate large oscillations of the total pressure. A typical sample of the distribution of the horizontal stresses along the side of the box is schown in fig. 7, the distribution is not hydrostatic as assumed by Mononobe.

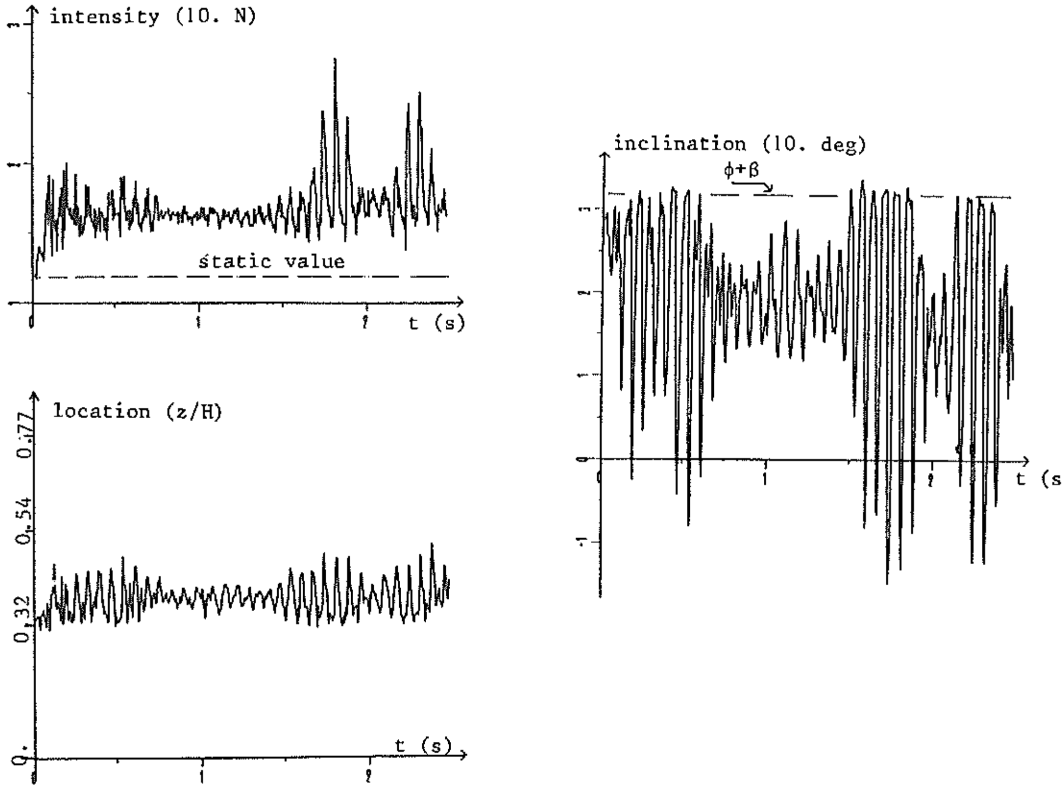

fig. 5 History of the total dynamic pressure against the gravity wall

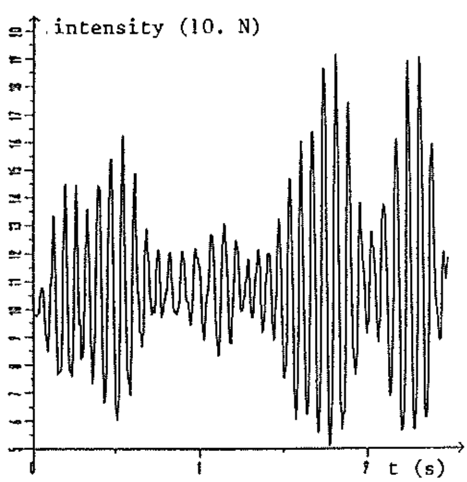

fig. 6 Total dynamic pressure against the fixed right side BC of the box.

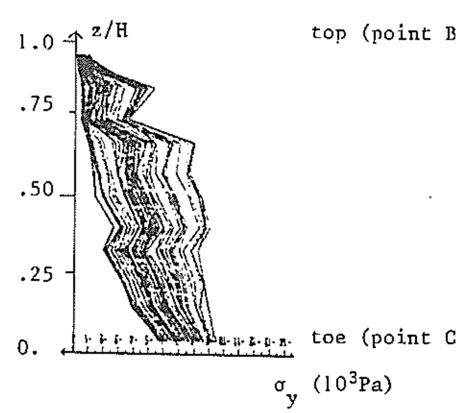

fig. 7 Distribution of horizontal stresses along the fixed side BC for 2.0 s $\leqq$ t $\leqq$ 2.5 s

5. CONCLUSION

With the proposed numrical tool it is possible to assess the validity of simplified procedures based on the Mononobe formula and to check different assumptions such as earth-pressure distribution during earthquakes or the position and inclination of the resultant force acting towards the retaining wall.

On the other way the numerical technique proposed here may be favourably extended to the study of the dynamic stability of slope and earthdam.

ACKNOWLEDGMENT

This research work has been undertaken under contract with Electricité de France/SEPTEN. This support is gratefully acknowledged.

REFERENCES

[1] NAZARIAN H.N., HADJIAN A.H. "Earthquake-induced soil pressures on structures" Journal Geotechnical Engineering, ASCE, 1979, Vol 105, GT 9, pp 1049-1066.

[2] MANDEL J. "Définition d'un repère privilégié pour l'étude des transformations anélastiques du polycristal". Journal de mécanique théorique et appliquée, 1982, Vol 1, N°1, pp 7-23.

[3] CHOUVET D. "Calcul dynamique élastoplastique d'interaction sol-structure. Application aux ouvrages de soutènement". Thèse de Docteur-Ingénieur - Ecole Centrale des Arts et Manufactures - PARIS - 1983.

[4] HUGHES T.J.R., LIU W.K. "Implicit-explicit finite elements in transient analysis". Journal of applied mechanics, 1978, Vol 45, pp 371-378.